0026-895X/05/6704-1009–1017$20.00
MOLECULAR PHARMACOLOGY
Copyright © 2005 The American Society for Pharmacology and Experimental Therapeutics
Mol Pharmacol 67:1009–1017, 2005

Vol. 67, No. 4
10793/1198127
Printed in U.S.A.

ACCELERATED COMMUNICATION

The New Anticonvulsant Retigabine Favors Voltage-Dependent Opening of the $K_v7.2$ (*KCNQ2*) Channel by Binding to Its Activation Gate

Thomas V. Wuttke, Guiscard Seebohm, Sigrid Bail, Snezana Maljevic, and Holger Lerche

Departments of Neurology and Applied Physiology, University of Ulm, Ulm, Germany (T.V.W., S.B., S.M., H.L.); and Department of Physiology, University of Tübingen, Tübingen, Germany (G.S.)

Received December 22, 2004; accepted January 19, 2005

ABSTRACT

Retigabine (RTG) is an anticonvulsant drug with a novel mechanism of action. It activates neuronal KCNQ-type K^+ channels by inducing a large hyperpolarizing shift of steady-state activation. To identify the structural determinants of KCNQ channel activation by RTG, we constructed a set of chimeras using the neuronal $K_v7.2$ (*KCNQ2*) channel, which is activated by RTG, and the cardiac $K_v7.1$ (*KCNQ1*) channel, which is not affected by this drug. Substitution of either the S5 or the S6 segment in $K_v7.2$ by the respective parts of $K_v7.1$ led to a complete loss of activation by RTG. Trp236 in the cytoplasmic part of S5 and the conserved Gly301 in S6 ($K_v7.2$), considered as the gating hinge (Ala336 in $K_v7.1$), were found to be crucial for the RTG effect: mutation of these residues could either knockout the effect in $K_v7.2$ or restore it partially in $K_v7.1/K_v7.2$ chimeras. We propose that RTG binds to a hydrophobic pocket formed upon channel opening between the cytoplasmic parts of S5 and S6 involving Trp236 and the channel's gate, which could well explain the strong shift in voltage-dependent activation.

Epilepsy is one of the most common neurological diseases, with a cumulative lifetime incidence of 3% (Hauser et al., 1996). Although 60 to 80% of patients with epilepsy respond well to treatment with available anticonvulsant drugs, approximately 30% are pharmacoresistent (Löscher, 1998). Therefore, there is a need to develop new anticonvulsants, which best should have mechanisms of action different from those currently in use, to enlarge the possibilities of differential treatment in mono- and polytherapy. Retigabine (RTG), a novel anticonvulsant, perfectly fulfills these criteria. Its main molecular mechanism of action is activation of the M current (Main et al., 2000; Rundfeldt and Netzer, 2000; Wickenden et al., 2000; Tatulian et al., 2001), a potassium conductance regulating the excitability in a wide variety of neuronal cells (Brown and Adams, 1980). None of the anticonvulsants that are in clinical use today has a comparable mechanism of action. RTG is effective in a broad range of epilepsy and seizure models (Rostock et al., 1996; Tober et al., 1996; Armand et al., 1999, 2000; Dost and Rundfeldt, 2000). In two models of drug-resistant epilepsy, it was the only compound able to antagonize hyperexcitability in a concentration-dependent manner (Armand et al., 1999, 2000) and was also effective in human brain slices derived from patients with pharmacoresistent epilepsy who underwent epilepsy surgery (Straub et al., 2001).

The M current is a slowly activating and noninactivating neuronal potassium conductance blocked via the activation of muscarinergic acetylcholine receptors (Brown and Adams, 1980). Its main molecular correlates are potassium channels of the KCNQ family (Wang et al., 1998). Five members have been cloned to date (genes: *KCNQ1–5*; proteins: $K_v7.1$–5) (Gutman et al., 2003), four of which (*KCNQ1–4*) are involved in hereditary diseases. These include a rare dominant form of epilepsy, benign familial neonatal convulsions, caused by mutations in *KCNQ2* and *KCNQ3* (Jentsch, 2000; Lerche et al., 2005). RTG activates the neuronal channels $K_v7.2$ to -5

This work was supported by grants of the Deutsche Forschungsgemeinschaft (DFG), Le1030/9-1, and of the Fritz-Thyssen-Stiftung (to H.L.). H.L. is a Heisenberg fellow of the DFG. T.V.W. was supported as a fellow by the graduate college GRK460 of the DFG.

Article, publication date, and citation information can be found at http://molpharm.aspetjournals.org.

doi:10.1124/mol.104.010793.

ABBREVIATIONS: RTG, retigabine; WT, wild type;

but not the cardiac $K_v7.1$ (Tatulian et al., 2001; Dupuis et al., 2002), which is an important prerequisite for the drug to avoid cardiac side effects. The main molecular mechanism of action is a large hyperpolarizing shift in the voltage-dependence of channel activation found for $K_v7.2$, $K_v7.3$, and $K_v7.5$. Therefore, RTG induces an opening of KCNQ channels at the resting membrane potential, shifting it toward the potassium equilibrium potential (E_K), a very powerful anticonvulsant mechanism.

The aim of our study was to identify the binding site of RTG in $K_v7.2$ channels and to reveal the molecular mechanism of channel activation. Chimeras systematically introducing different parts of $K_v7.1$ into $K_v7.2$ revealed that RTG binds within the pore region. More detailed experiments, using point mutations in both channels and certain chimeras, indicated that RTG stabilizes the open-pore conformation by binding to the channel's activation gate between the cytoplasmic parts of the S5 and S6 segments. The structure of bacterial potassium channels (Doyle et al., 1998; Jiang et al., 2002) was then used to develop a model for the potential binding site, suggesting a binding pocket formed by the open channel's S5 and S6 segments.

Materials and Methods

Mutagenesis and RNA Preparation. Chimeras of *KCNQ1* and *KCNQ2* cDNAs were constructed by using unique restriction sites inserted in both channels at corresponding positions (Fig. 1): a SacI site at the cytoplasmic end of S5 (Glu231/Leu232 in $K_v7.2$), a XhoI site in the membrane part of S5 (Ala246/Ser247/Phe248 in $K_v7.2$), an NsiI site at the beginning of H5 (Asp266/Ala267/Leu268 in $K_v7.2$), a KpnI site at the end of H5 (Lys283/Tyr284/Pro285 in $K_v7.2$), and a BamHI site at the cytoplasmic end of S6 (Gly313/Ser314 in $K_v7.2$). Additional chimeras exchanging S1/S2, S3/S4, and S4/S4–S5, as well as point mutations, were introduced using recombinant polymerase chain reaction techniques. Mutants were assembled in either the pTLN or the pSGEM vector and verified by automated DNA sequencing. DNA was in vitro-transcribed using the SP6 or the T7 mMessage mMachine kit (Ambion, Austin, TX), resulting in capped cRNA. Purity was checked by gel electrophoresis.

Oocyte Preparation and Injection. All procedures met the National Institute of Health guidelines for the care and use of laboratory animals and were approved by the Regierungspraesidium Tuebingen, Germany. Tricaine (0.1%; Sigma Chemie, Deisenhofen, Germany) was used to anesthetize female *Xenopus laevis* frogs. Oocytes were obtained surgically and immediately treated for 2 h by collagenase (2 mg/ml type CLS III collagenase; Biochrom, Berlin, German) in OR2 solution (82.5 mM NaCl, 2.5 mM KCl, 1 mM $MgCl_2$ and 5 mM HEPES, pH 7.6) to remove follicular structures. Defolliculated oocytes were stored at 18°C in frog Ringer's solution (115 mM NaCl, 2.5 mM KCl, 1.8 mM $CaCl_2$, and 10 mM HEPES, pH 7.4) supplemented with 1% fetal calf serum and 50 μg/ml gentamicin (Biochrom). Diluted cRNA (10–20 ng) was injected into each oocyte within 24 h after preparation. Electrophysiological measurements were performed 2 to 5 days after injection.

Fig. 1. Alignment of the pore regions of $K_v7.1$ to -5 (*KCNQ1–5*), Shaker, KcsA, and MthK channels. Black letters indicate conserved amino acids, and gray letters represent divergent amino acids within the channel sequences. S5 and S6 are transmembrane segments, H5 the loop containing the selectivity filter.

Electrophysiology. Potassium currents were recorded using standard two-microelectrode voltage clamp, a Turbo TEC01C amplifier (NPI Electronic GmbH, Tamm, Germany) and pClamp data acquisition (Axon Instruments Inc., Union City, CA), as described previously (Lerche et al., 1999). Frog Ringer's solution (see above) was used as the bathing solution for all recordings. RTG was dissolved in dimethyl sulfoxide to obtain 1000-fold concentrated stock solutions for final concentrations of 0.1, 1, 10, and 100 μM. Aliquots of each concentration were stored at −20°C, unfrozen, and directly diluted in frog Ringer's solution on the day electrophysiological experiments were performed. The maximal concentration of dimethyl sulfoxide did not exceed 1 ml per 100 liters.

Recording electrodes were filled with 3 M KCl and had a resistance of 0.3 to 1 MΩ. Oocytes had resting membrane potentials between −30 and −75 mV. Currents were low-pass–filtered at 0.3 kHz and sampled at 1 kHz. Oocytes were clamped to a membrane potential of −100 mV followed by depolarizing 20-mV steps up to +20 mV. Tail currents were measured at −30 mV, and their amplitudes were analyzed to obtain conductance-voltage plots. To obtain dose-response curves for RTG, oocytes were superfused with increasing concentrations of RTG (0.1, 1, 10, and 100 μM) using a homemade multibarrel application system.

Data were analyzed using pClamp, Microsoft Excel (Microsoft, Redmond, WA), and Origin (OriginLab Corp., Northampton, MA) software. For statistical evaluation, Student's t test was applied. All data are shown as means ± S.E.M. Conductance-voltage curves are fit to the Boltzmann equation $I/I_{max}(V) = 1/(1 + \exp[(V - V_{0.5})/k])$, where I/I_{max} is the normalized tail current amplitude, $V_{0.5}$ is the voltage of half-maximal activation, and k is a slope factor. All semi-logarithmic plots of RTG response against RTG concentration represent fits to a logistic (or Hill) function according to the following equation: Response $= A_2 + [(A_1 - A_2)/(1 + (x/x_0)^{n_H})]$, where A_1 is the initial response, A_2 the final response, x is the drug concentration, x_0 is the EC_{50}, and n_H is the slope (Hill coefficient) of the curve.

Modeling. The MthK channel structure (1LNQ) and the KcsA channel structure (1BL8) were retrieved from the Protein Data Bank. A three-dimensional structural model of the S5 to S6 domains of $K_v7.2$ were constructed on the basis of homology to MthK/KscA using the solved crystal structures of the corresponding domains. The $K_v7.2$ models were generated using SWISS-MODEL (http://www.expasy.org/swissmod/SWISS-MODEL.html) and were energy-optimized using Gromos96 in default settings within the Swiss-PdbViewer (Guex and Peitsch, 1997). Manual docking of eight energy-optimized RTG conformers (ACD/Chemsketch; Advanced Chemistry Development, Inc., Toronto, ON, Canada) in the $K_v7.2$ homology models were performed. The resulting model was subsequently energy-optimized using Gromos96. The model with the most likely binding conformation is represented here.

Results

Wild-type (WT) and mutant/chimeric $K_v7.1$ and $K_v7.2$ channels were heterologously expressed in *X. laevis* oocytes and functionally characterized using two-microelectrode voltage clamping. RTG was applied extracellularly by adding it to the bathing solution in increasing concentrations of 1, 10, and 100 μM.

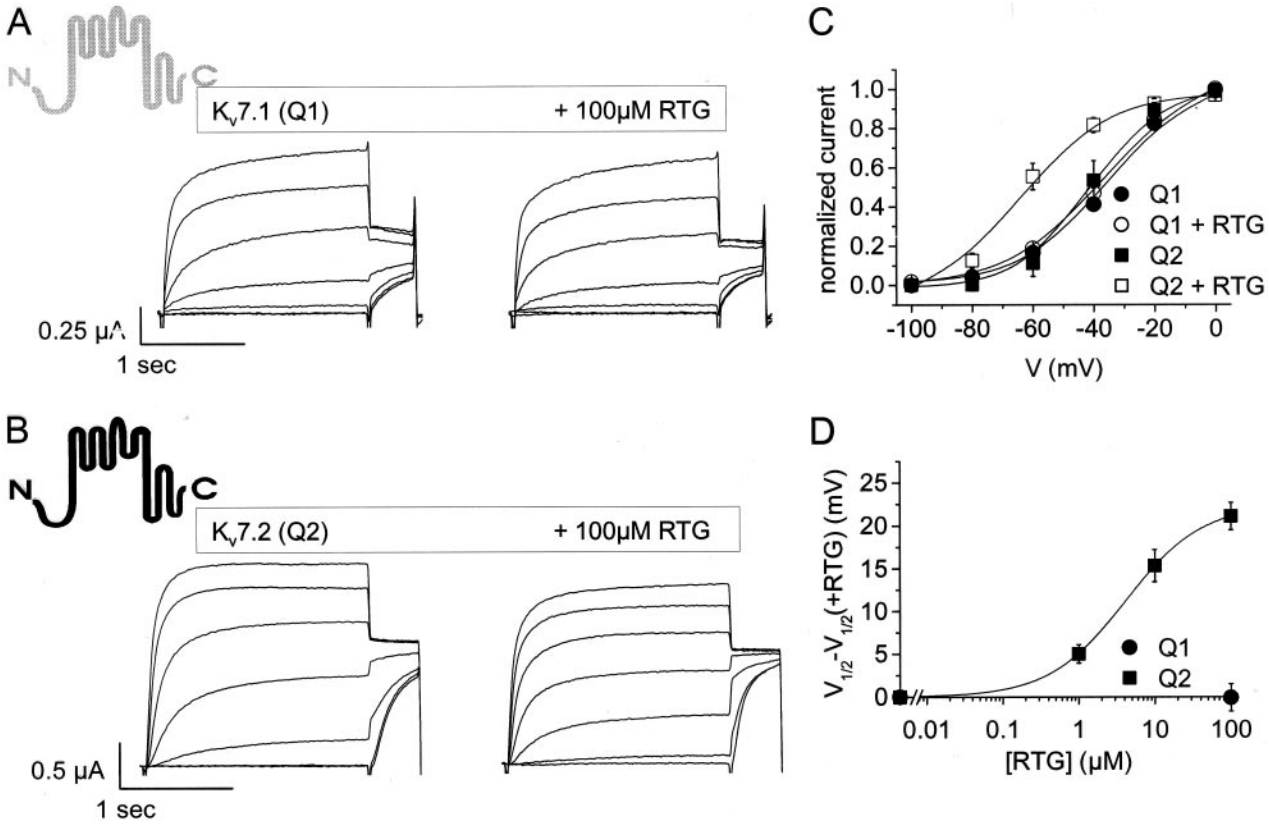

Fig. 2. Effects of RTG (100 μM) on $K_v7.1$ WT and $K_v7.2$ WT channels. A and B, raw current traces elicited from a holding potential of −100 mV by depolarizations ranging from −100 to +20 mV in 20-mV steps before and after the application of RTG. Note the slight decrease in current amplitude observed for both channels. C, conductance-voltage curves were constructed by plotting the normalized tail current amplitude against the membrane potential. The lines represent fits of a Boltzmann equation to the data points (see *Materials and Methods*) showing a leftward shift of the KCNQ2 activation curve after application of 100 μM RTG. The KCNQ1 activation curve remains unaffected. D, dose-response curve for channel activation by RTG. The relative shift in voltage dependence is plotted against the RTG concentration. The line represents a fit to the Hill equation (see *Materials and Methods*). Data are shown as mean ± S.E.M., $n = 5$ to 6.

Effects of RTG on $K_v7.1$ and $K_v7.2$ WT Channels. Effects of RTG on currents conducted by $K_v7.1$ and $K_v7.2$ channels are shown in Fig. 2. The drug had no significant effect on the voltage dependence of activation of WT $K_v7.1$ channels (Fig. 2C), but in a concentration of 100 μM, it slightly reduced current amplitudes (Fig. 2A) (Tatulian et al., 2001). In contrast, the voltage dependence of steady-state activation of WT $K_v7.2$ channels was largely shifted toward more negative membrane potentials upon application of increasing concentrations of RTG. The EC_{50} value was determined to be 4.1 μM with a Hill coefficient of 0.88, suggesting that one RTG molecule is sufficient to exert this activating effect on a single $K_v7.2$ channel (Fig. 2D). RTG in a concentration of 100 μM reduced the maximal $K_v7.2$ current amplitude, similar to that for $K_v7.1$ (Figs. 2B and 5A), which was in line with previous observations suggesting that an increase of the current amplitude for $K_v7.2$ by RTG was limited at strongly positive potentials (Tatulian et al., 2001). Kinetics of deactivation of $K_v7.2$ were significantly slowed by RTG, as was described by other groups previously for $K_v7.2/3$ coexpression (Main et al., 2000; Wickenden et al., 2000). A first-order exponential was fit to the deactivation time course at potentials between −80 and −120 mV. The time constants at −110 mV were 67 ± 5 ms before and 219 ± 31 ms after application of 100 μM RTG ($p < 0.01$, $n = 4$).

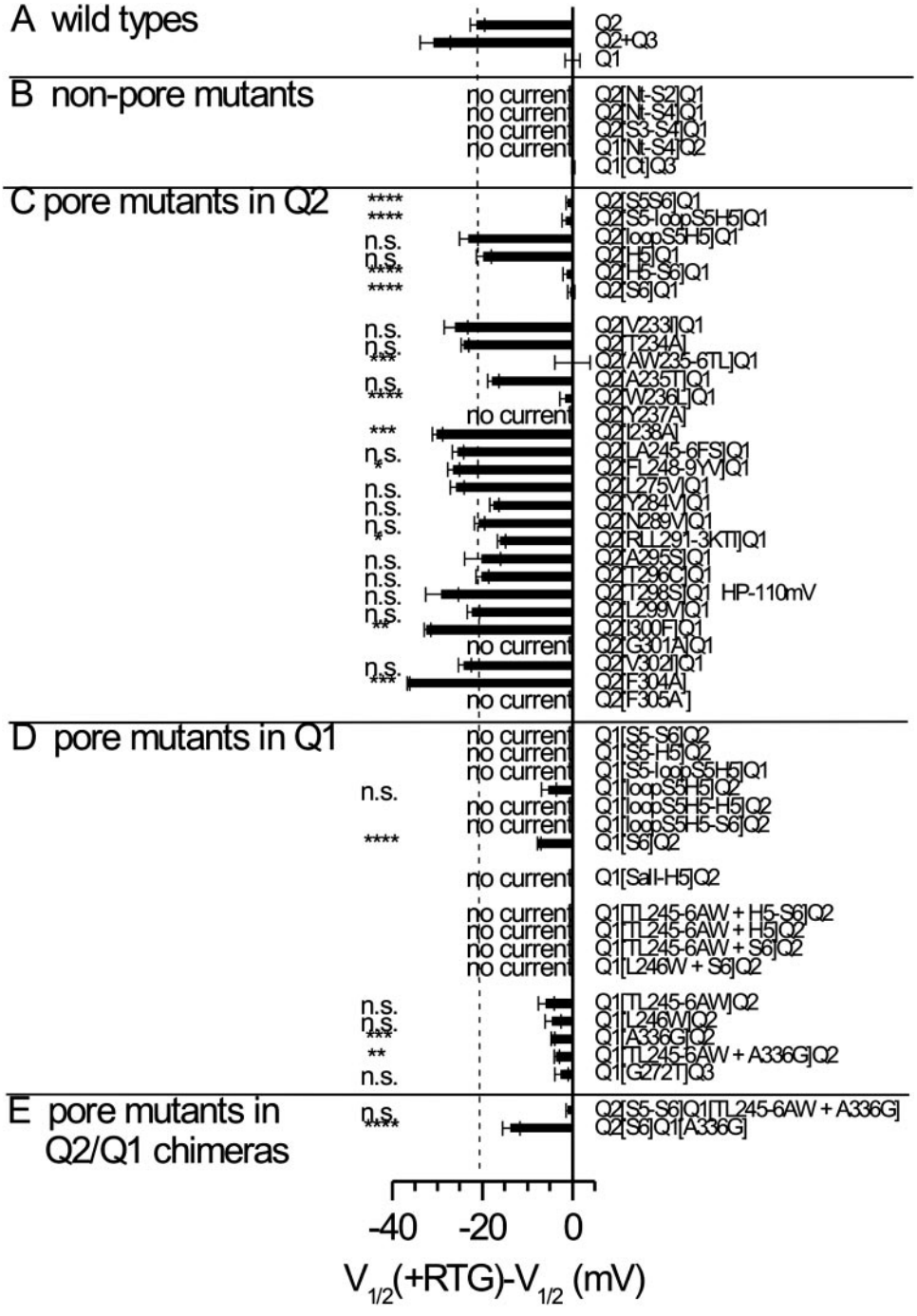

Fig. 3. Summary of RTG effects for all mutants investigated. Shifts of activation curves upon application of 100 μM RTG are plotted as mean ± S.E.M. (n = 3–12). The broken line indicates the shift for $K_v7.2$ (Q2). Student's t test was applied to evaluate the significance of either the reduction (C) or the introduction (D and E) of the shift. Different levels of significance are represented by: n.s., not significant; ⋆, $p < 0.05$; ⋆⋆, $p < 0.01$; ⋆⋆⋆, $p < 0.001$; ⋆⋆⋆⋆, $p < 0.0001$; no current, a nonfunctional channel construct.

Analysis of $K_v7.2/K_v7.1$ Chimeras. To determine protein regions involved in the effect of RTG, we constructed a set of chimeras substituting different parts of $K_v7.2$ with the respective sequences of $K_v7.1$ (nomenclature for these chimeras, Q2[channel region]Q1; for example Q2[Cterm]Q1′ would signify a $K_v7.2$ channel containing a C terminus of $K_v7.1$, or Q2[Nterm-S4]Q1′ for a chimera built of N terminus and S1–S4 segments from $K_v7.1$ but S5–S6 segments and C terminus of $K_v7.2$). All constructed chimeras substituting parts of segments S1 to S4 were nonfunctional (Q2[Nterm-S4]Q1, Q2[Nterm-S2]Q1, Q2[S3-S4]Q1, and Q1[Nterm-S4]Q2). Exchange of the C terminus (Q2[Cterm]Q1) did not significantly change the RTG effect, but substitution of the whole-pore region (Q2[S5–S6]Q1) completely abolished channel activation by RTG (Figs. 3 and 4). To further narrow the relevant sequences for the RTG effect, we dissected the pore region into four parts by introducing silent restriction sites (see *Materials and Methods*; Fig. 1). For the chimeras Q2[S5-loopS5H5]Q1, substituting the S5 segment and extracellular loop between S5 and H5 (SacI-NsiI), Q2[H5-S6]Q1 (NsiI-BamHI), and Q2[S6]Q1 (KpnI-BamHI), channel activation was also not observed using up to 100 μM RTG. In contrast, the reaction upon application of RTG was not significantly changed for Q2[loopS5H5]Q1 (XhoI-NsiI) and Q2[H5]Q1 (NsiI-KpnI) compared with $K_v7.2$ WT channels (Figs. 3 and 4). These results suggest an RTG binding site within the S5 and S6 segments not involving the selectivity filter or the extracellular pore loops.

Effects of Point Mutations in $K_v7.2$ on RTG Sensitivity. Within the largely conserved pore region, there are only few residues that are different in $K_v7.1$ compared with $K_v7.2$ to -5 (Fig. 1). At these sites, we introduced point mutations in $K_v7.2$, substituting the respective amino acids from $K_v7.1$. In the S6 segment, the most intriguing alteration of the $K_v7.1$ sequence is a change of the highly conserved glycine 301, which is supposed to function as the gating hinge in a large spectrum of potassium channels, including the *Shaker* channel; the bacterial channels KcsA, MthK, and K_vAP (Jiang et

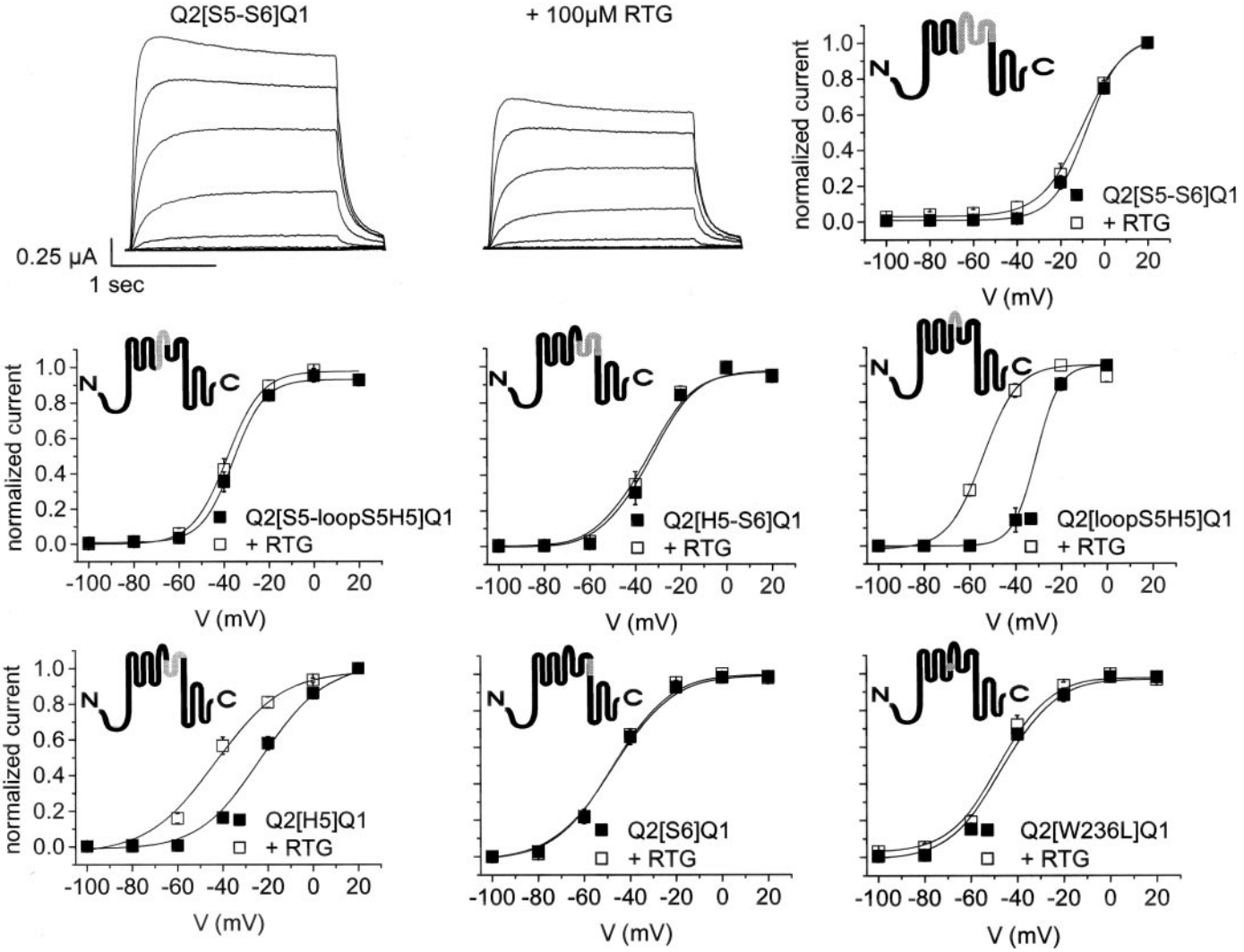

Fig. 4. Knockout of the RTG effect in $K_v7.2$. Conductance-voltage plots were generated for Q2/Q1 chimeras ($n = 4–7$) exchanging different parts within the pore region (S5–S6 segments) before and after application of 100 μM RTG. Exchange of the whole [S5–S6] segment as well as the exchange of the [S5-loopS5H5], [H5S6], [S6] segments or the amino acid [W236L] abolished the RTG-induced leftward shift of the activation curve. However, RTG still reduces the current amplitude of the Q2[S5–S6]Q1 mutant, as already observed for both WT channels (Fig. 2). The leftward shift of Q2[H5]Q1 and Q2[loopS5H5]Q1 is not significantly reduced compared with $K_v7.2$. Data were obtained as described in the legend to Fig. 2 and in *Materials and Methods*.

al., 2002); and even a bacterial sodium channel (Zhao et al., 2004). Mutation of Gly301 in $K_v7.2$ to an alanine, the corresponding amino acid in $K_v7.1$ (Q2[G301A]Q1), resulted in a nonfunctional channel, confirming the importance of this residue for channel gating in $K_v7.2$ channels. Some other S6 mutations showed little but significant alterations of the modification by RTG (e.g., a reduction of the negative shift by Q2[RLL291–3KTI]Q1) (see summary in Fig. 3).

In S5, the double mutation Q2[AW235–6TL]Q1 as well as the single mutation Q2[W236L]Q1 completely knocked out the RTG effect, whereas all other mutations did not change the reaction to RTG. Because Trp236 is located at the cytoplasmic end of S5, this result, together with the knockout of the RTG effect by substitution of the S6 segment, strongly suggests a binding of RTG to the cytoplasmic parts of S5 and S6 segments involving the channel's activation gate, which is supposed to be formed by residues downstream of the putative gating hinge Gly301. To identify further residues in these two protein regions, we mutated a few amino acids around Trp236 in S5 and the hydrophobic phenylalanines 304/305 in S6 to alanines, because RTG is highly lipophilic and therefore is supposed to bind to lipophilic residues in KCNQ channels. Q2[F304A] and Q2[I238A] showed a significantly increased sensitivity to RTG, whereas Q2[F305A] and Q2[Y237A] did not lead to functional channels. Q2[T234A] did not change the RTG effect significantly (Fig. 3).

Introduction of the RTG Binding Site in $K_v7.1$ or $K_v7.1/K_v7.2$ Chimeras. To evaluate the importance of Trp236 and Gly301 for the RTG effect, we introduced these residues in $K_v7.1$ and tested their impact on RTG sensitivity. For Q1[TL245–6AW]Q2 and Q1[L246W]Q2, the maximum effect of RTG on the voltage dependence of steady-state activation was a −5 mV shift (Fig. 3), but there was no clear relationship to the RTG concentration, so these small alterations have to be interpreted with caution. However, for Q1[L246W]Q2, we observed a strong, concentration-dependent reduction in current amplitude by RTG that was not

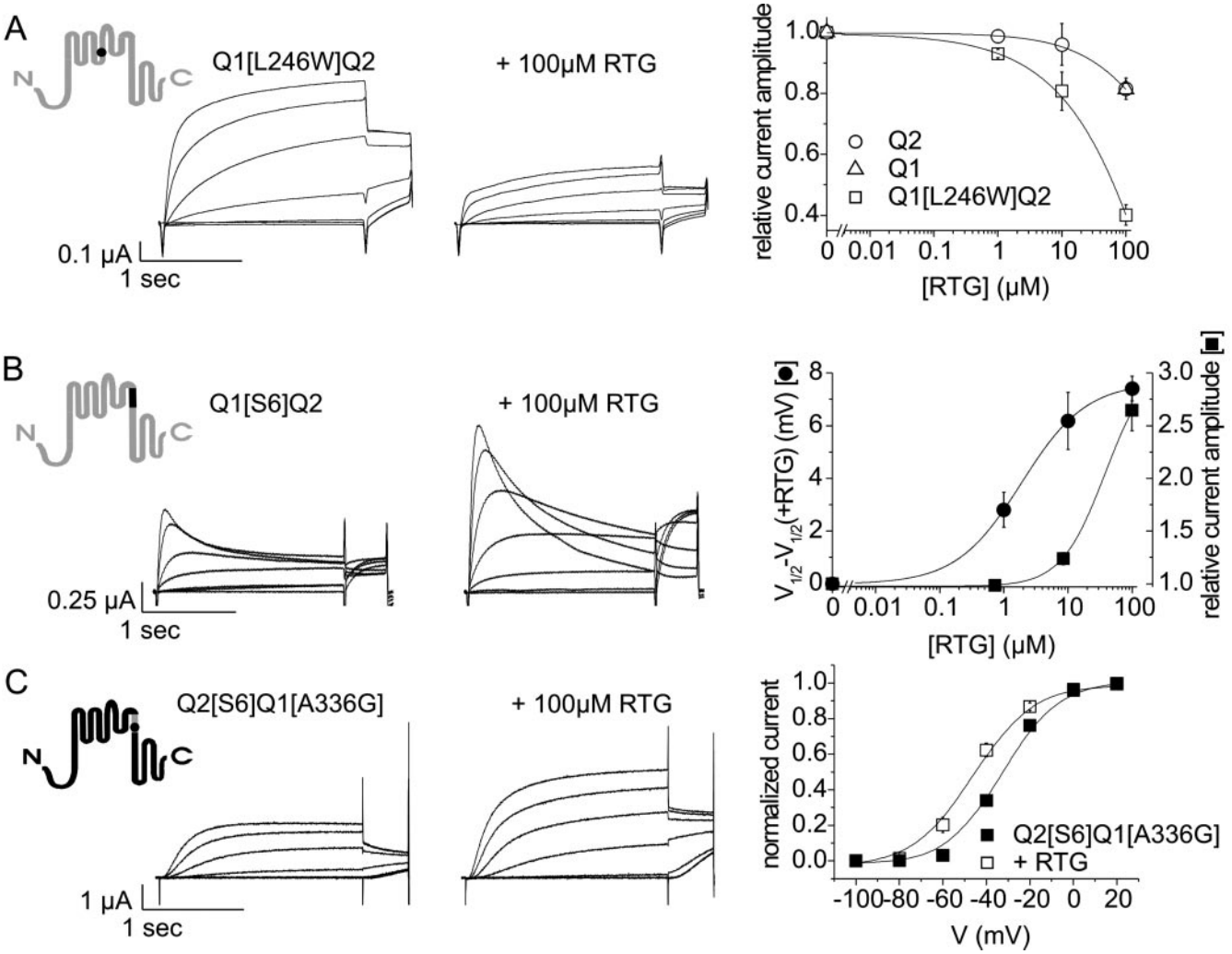

Fig. 5. Knock-in of RTG effects in $K_v7.1$ or $K_v7.1/K_v7.2$ chimeras. A, according to the displayed raw current traces, RTG strongly reduces the current amplitude of Q1[L246W]Q2. Plotting the relative current amplitude against the RTG concentration reveals a clear concentration-dependence of the current reduction (n = 4–5). Q1 was only measured for 100 µM RTG. The lines represent fits of the Hill equation to the data points (see *Materials and Methods*). B, current traces of Q1[S6]Q2 show both an increase in current amplitude and a leftward shift of voltage-dependent activation induced by RTG (100 µM). The clear concentration-dependence for both effects is shown in the right diagram (n = 5). The lines represent fits to the Hill equation (see *Materials and Methods*). C, current traces and conductance-voltage plots of Q2[S6]Q1[A336G] reveal an RTG-induced leftward shift of the activation curve (n = 12) and an increase in current amplitude. In contrast, no shift was observed for Q2[S6]Q1 (compare with Fig. 4). Data were obtained as described in the legend to Fig. 2 and in *Materials and Methods*.

observed to this extent for $K_v7.1$ or $K_v7.2$ (Figs. 5A and 2A), indicating that introduction of the tryptophan in this position increased this drug effect.

Introduction of a glycine at the corresponding hinge position in $K_v7.1$ (Q1[A336G]Q2) resulted in larger currents than observed for $K_v7.1$ WT channels, but we did not observe a significant effect of RTG. We did not observe stronger effects of RTG when both of these changes in S5 and S6 were simultaneously introduced into $K_v7.1$ (Fig. 3). Because the overall pore structures of $K_v7.1$ and $K_v7.2$ channels might be quite different, introduction of single amino acids may not be sufficient to induce a large RTG effect in $K_v7.1$. We therefore exchanged the whole S6 segment (Q1[S6]Q2). It is interesting to note that this chimera showed a clear RTG sensitivity; however, it revealed a different effect on channel gating than was observed for $K_v7.2$. Although the shift of the voltage dependence of activation was relatively small (−7.4-mV shift), a concentration-dependent, almost 3-fold increase in current amplitude was observed upon application of RTG (Fig. 5B). We next tried to combine Q1[S6]Q2 with Q1[L246W]Q2 and Q1[TL245–6AW]Q2, but these chimeras were nonfunctional, further suggesting considerable differences of the pore structures and gating mechanisms of $K_v7.1$ and $K_v7.2$. To further investigate the importance of the gating hinge for the RTG sensitivity, we constructed a chimera of $K_v7.2$ having an S6 segment of $K_v7.1$ with a glycine in position 336 ($K_v7.1$ numbering): Q2[S6]Q1[A336G]. For this mutation, the RTG-induced shift in voltage dependence—which was completely abolished in Q2[S6]Q1 (Fig. 4)—was largely restored (−13.6 mV shift), and current amplitudes were also significantly increased (Figs. 3 and 5C). These alterations strongly suggest a crucial role of the predicted flexibility of the S6 segment at the glycine hinge for RTG binding in $K_v7.2$ channels.

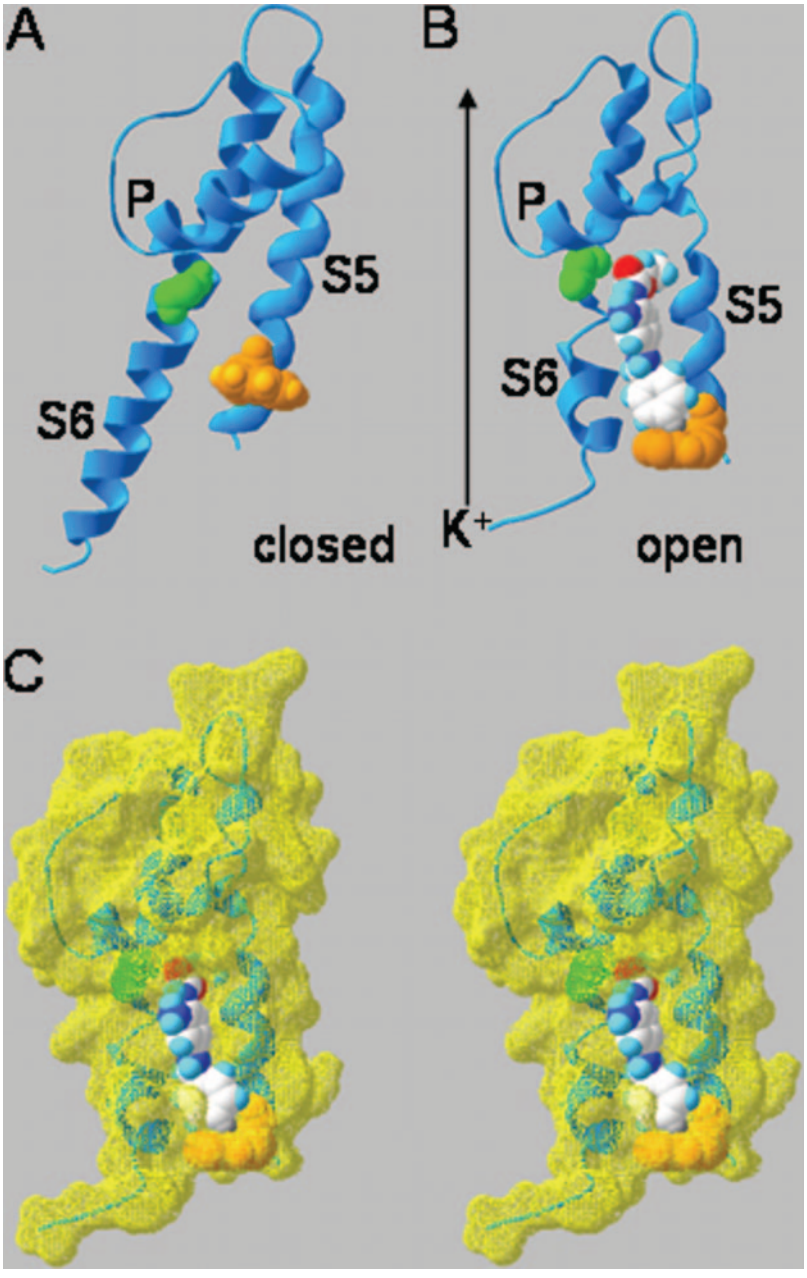

Fig. 6. Computer model for the binding of the RTG molecule within the pore region of the $K_v7.2$ (*KCNQ2*) channel. Shown are energy-optimized homology models of the $K_v7.2$ pore domain derived from the crystal structures of KscA (A, closed conformation) and MthK (B, open conformation). The glycine in position 301, serving as a putative gating hinge, is shown in green, and the tryptophan in position 236, in orange. The RTG molecule was manually docked in the open channel (B) (see *Materials and Methods* for details). C, stereoview of B, including a reconstruction of the protein surface (in yellow).

Discussion

Two lines of evidence emerging from our results suggest that the cytoplasmic parts of S5 and S6 segments form the binding site for RTG. First, our results reveal that two amino acids located in these two helices play crucial roles for the activation of $K_v7.2$ by RTG: a tryptophan residue at the cytoplasmic end of S5, Trp236, and the gating hinge in S6, Gly301. To correlate these functional results to the possible structure of the channel, we developed homology models of the S5 to S6 region of $K_v7.2$ for both the closed and the open state, which were derived from the crystal structures of the KcsA (closed conformation, Doyle et al., 1998) and the MthK (open conformation, Jiang et al., 2002) channels (for details, see *Materials and Methods*). As shown in Fig. 6, comparison of both channel conformations suggested the formation of a hydrophobic pocket between the cytoplasmic parts of S5 and S6 upon opening of the channel in which the energy-optimized RTG molecule could be docked manually. The pocket was induced by a kinking of the S6 helix at the gating hinge and a simultaneous conformational change of S5 (Fig. 6, B and C). In contrast, the parallel orientation of the S5 and S6 helices of the closed channel would not allow RTG binding (Fig. 6A). This model predicts a specific lipophilic interaction between the fluorophenyl ring of RTG and the aromatic Trp236 (Fig. 6B), which perfectly matches our electrophysiological experiments knocking out the RTG effect in $K_v7.2$ by the point mutation Q2[W236L]Q1. Furthermore, the model illustrates the importance of the flexibility of the S6 helix at the gating hinge (Gly301) to form the binding pocket, as was functionally suggested 1) by the knock-in of an RTG effect by introducing the complete S6 segment of $K_v7.2$ into $K_v7.1$ and particularly 2) by introducing a glycine at the gating hinge into the chimera Q2[S6]Q1. Furthermore, the relative increase of RTG sensitivity of the mutant Q2[F304A] underlines the importance of the helix distal to Gly301. Nevertheless, this computed model has to be interpreted with caution, because the RTG molecule is rather flexible and because the modeling revealed a considerable variability, particularly in the more cytoplasmic regions, when we tried to adapt the putative structure of $K_v7.2$ to the ones of KscA or MthK.

A second supporting evidence for an RTG binding site between the cytoplasmic parts of S5 and S6 segments derives from the biophysical mechanism of $K_v7.2$ activation. The large hyperpolarizing shift of the voltage dependence of steady-state activation can be well explained by a stabilization of the open-gate conformation induced by RTG binding in this channel region. In general, such a shift in voltage dependence is likely to result either from a direct effect on the voltage sensor or alternatively from affecting its coupling to the opening of the pore (i.e., the activation gate). A nice example for the latter possibility was given in a recent study by Zhao et al. (2004). When the glycine, considered to be the gating hinge in the S6 segment of a bacterial sodium channel, was replaced by a proline, which disrupts the α-helical structure and reduces its flexibility, voltage-dependent activation of the channel was shifted by -51 mV. In *Shaker* potassium channels, large parallel shifts in the voltage dependence of channel activation by mutations at the gate have been observed (Hackos et al., 2002). Thus, the hyperpolarizing shift induced by RTG would be very well compatible with the hypothesis that RTG binds in between the S5 and S6 segments, involving the gate itself, thereby stabilizing the open channel conformation. In addition, the slowing of the deactivation time course by RTG could be well explained if RTG binds to the activation gate. The alterations in current amplitudes as observed for some of the mutants could be caused by decreases or increases in single-channel conductance, which would also fit well with the hypothesis of RTG binding in the pore region. For a discussion of the inactivation occurring in Q1[S6]Q2 see Seebohm et al. (2001).

Activation of a potassium channel at the resting membrane potential, as has been demonstrated for RTG (Main et al., 2000; Rundfeldt and Netzer, 2000; Wickenden et al., 2000; and this study), is a very potent anticonvulsant mechanism, because the resting potential is stabilized toward the potassium equilibrium potential (E_K). None of the anticonvulsants that are in clinical use today exhibits such a mechanism of action. The efficacy of RTG has been shown in a large variety of seizure models (Rostock et al., 1996; Tober et al., 1996; Armand et al., 1999, 2000; Dost and Rundfeldt, 2000). Therefore, RTG, its derivatives, or other compounds with similar effects on neuronal potassium channels of the KCNQ family could be used as powerful drugs in the future treatment of epilepsy or other disorders going along with a membrane depolarization and hyperexcitability of the nervous system such as migraine, neuropathic pain, and stroke. Elucidation of the molecular mechanism of action of such compounds, as shown here for RTG, will contribute to a better understanding of drug-receptor interactions and should help to develop more specific and more effective drugs with fewer side effects.

Acknowledgments

We thank Viatris GmbH and Co. KG, Radebeul, Germany, and Xcel Pharmaceuticals, San Diego, CA, for providing Retigabine. Furthermore, we thank Dr. Thomas Jentsch for providing the human KCNQ2 and KCNQ3 cDNA, Dr. Christian Lerche for providing some of the chimeric channels, Dr. Stephan Grissmer for reading through the manuscript, and Astrid Bellan-Koch for technical support.

References

Armand V, Rundfeldt C, and Heinemann U (1999) Effects of retigabine (D-23129) on different patterns of epileptiform activity induced by 4-aminopyridine in rat entorhinal cortex hippocampal slices. *Naunyn Schmiedebergs Arch Pharmacol* **359:**33–39.

Armand V, Rundfeldt C, and Heinemann U (2000) Effects of retigabine (D-23129) on different patterns of epileptiform activity induced by low magnesium in rat entorhinal cortex hippocampal slices. *Epilepsia* **41:**28–33.

Brown DA and Adams PR (1980) Muscarinic suppression of a novel voltage-sensitive K^+ current in a vertebrate neurone. *Nature (Lond)* **283:**673–676.

Dost R and Rundfeldt C (2000) The anticonvulsant retigabine potently suppresses epileptiform discharges in the low Ca^{++} and low Mg^{++} model in the hippocampal slice preparation. *Epilepsy Res* **38:**53–66.

Doyle DA, Morais Cabral J, Pfuetzner RA, Kuo A, Gulbis JM, Cohen SL, Chait BT, and MacKinnon R (1998) The structure of the potassium channel: molecular basis of K^+ conduction and selectivity. *Science (Wash DC)* **280:**69–77.

Dupuis DS, Schroder RL, Jespersen T, Christensen JK, Christophersen P, Jensen BS, and Olesen SP (2002) Activation of KCNQ5 channels stably expressed in HEK293 cells by BMS 204352. *Eur J Pharmacol* **437:**129–137.

Guex N and Peitsch MC (1997) SWISS-MODEL and the Swiss-PdbViewer: an environment for comparative protein modeling. *Electrophoresis* **18:**2714–2723.

Gutman GA, Chandy KG, Adelman JP, Aiyar J, Bayliss DA, Clapham DE, Covarriubias M, Desir GV, Furuichi K, Ganetzky B, et al. (2003) International Union of Pharmacology. International Union of Pharmacology. XLI. Compendium of voltage-gated ion channels: potassium channels. *Pharmacol Rev* **55:**583–586.

Hackos DH, Chang TH, and Swartz KJ (2002) Scanning the intracellular S6 activation gate in the shaker K^+ channel. *J Gen Physiol* **119:**521–532.

Hauser WA, Annegers JF, and Rocca WA (1996) Descriptive epidemiology of epi-

lepsy: contributions of population-based studies from Rochester, Minnesota. *Mayo Clin Proc* **71:**576–586.
Jentsch TJ (2000) Neuronal KCNQ potassium channels: physiology and role in disease. *Nat Rev Neurosci* **1:**21–30.
Jiang Y, Lee A, Chen J, Cadene M, Chait BT, and MacKinnon R (2002) The open pore conformation of potassium channels. *Nature (Lond)* **417:**523–526.
Lerche H, Biervert C, Alekov AK, Schleithoff L, Lindner M, Klinger W, Bretschneider F, Mitrovic N, Jurkat-Rott K, Bode H, et al. (1999) A reduced K^+ current due to a novel mutation in KCNQ2 causes neonatal convulsions. *Ann Neurol* **46:**305–312.
Lerche H, Weber YG, Jurkat-Rott K, and Lehmann-Horn F (2005) Ion channel defects in idiopathic epilepsies. *Curr Pharm Des*, in press.
Löscher W (1998) New visions in the pharmacology of anticonvulsion. *Eur J Pharmacol* **342:**1–13.
Main MJ, Cryan JE, Dupere JR, Cox B, Clare JJ, and Burbidge SA (2000) Modulation of KCNQ2/3 potassium channels by the novel anticonvulsant retigabine. *Mol Pharmacol* **58:**253–262.
Rostock A, Tober C, Rundfeldt C, Bartsch R, Engel J, Polymeropoulos EE, Kutscher B, Loscher W, Honack D, White HS, et al. (1996) D-23129: a new anticonvulsant with a broad spectrum activity in animal models of epileptic seizures. *Epilepsy Res* **23:**211–223.
Rundfeldt C and Netzer R (2000) The novel anticonvulsant retigabine activates M-currents in Chinese hamster ovary-cells transfected with human KCNQ2/3 subunits. *Neurosci Lett* **282:**73–76.
Seebohm G, Scherer CR, Busch AE, and Lerche C (2001) Identification of specific pore residues mediating KCNQ1 inactivation. A novel mechanism for long QT syndrome. *J Biol Chem* **276:**13600–13605.
Straub H, Kohling R, Hohling J, Rundfeldt C, Tuxhorn I, Ebner A, Wolf P, Pannek H, and Speckmann E (2001) Effects of retigabine on rhythmic synchronous activity of human neocortical slices. *Epilepsy Res* **44:**155–165.
Tatulian L, Delmas P, Abogadie FC, and Brown DA (2001) Activation of expressed KCNQ potassium currents and native neuronal M-type potassium currents by the anticonvulsant drug retigabine. *J Neurosci* **21:**5535–5545.
Tober C, Rostock A, Rundfeldt C, and Bartsch R (1996) D-23129: a potent anticonvulsant in the amygdala kindling model of complex partial seizures. *Eur J Pharmacol* **303:**163–169.
Wang HS, Pan Z, Shi W, Brown BS, Wymore RS, Cohen IS, Dixon JE, and McKinnon D (1998) KCNQ2 and KCNQ3 potassium channel subunits: molecular correlates of the M-channel. *Science (Wash DC)* **282:**1890–1893.
Wickenden AD, Yu W, Zou A, Jegla T, and Wagoner PK (2000) Retigabine, a novel anti-convulsant, enhances activation of KCNQ2/Q3 potassium channels. *Mol Pharmacol* **58:**591–600.
Zhao Y, Yarov-Yarovoy V, Scheuer T, and Catterall WA (2004) A gating hinge in Na^+ channels: a molecular switch for electrical signaling. *Neuron* **41:**859–865.

Address correspondence to: Dr. Holger Lerche, Neurologische Klinik/Abteilung Angewandte Physiologie, Universität Ulm, Zentrum Klinische Forschung, Helmholtzstr. 8/1, 89081 Ulm, Germany. E-mail: holger.lerche@medizin.uni-ulm.de